

Stability and Convergence of a Randomized Model Predictive Control Strategy

Daniël W. M. Veldman, Alexandra Borkowski, and Enrique Zuazua

Abstract—RBM-MPC is a computationally efficient variant of Model Predictive Control (MPC) in which the Random Batch Method (RBM) is used to speed up the finite-horizon optimal control problems at each iteration. In this paper, stability and convergence estimates are derived for RBM-MPC of unconstrained linear systems. The obtained estimates are validated in a numerical example that also shows a clear computational advantage of RBM-MPC.

Index Terms—Error Estimates, Model Predictive Control, Random Batch Method, Receding Horizon Control, Stability

I. INTRODUCTION

Model Predictive Control (MPC) is a well-established and widely used method to control complex dynamical systems, see, e.g., [1], [2], [3] for an overview of the large body of research in this area. MPC requires the real-time solution of a sequence of optimal control problems (OCPs) on a finite (but large) time horizon, which can be computationally demanding. This is for example the case when the model is the result of the (spatial) discretization of a Partial Differential Equation (PDE) or in the simulation of interaction particle systems.

One recently-proposed numerically-efficient approximation method is the Random Batch Method (RBM) [4], which is closely related to the stochastic algorithms like Stochastic Gradient Descent (SGD). In the RBM-dynamics, a random subset/batch of interconnections between Degrees of Freedom (DOFs) is considered during small time intervals. This can reduce the computational cost significantly and leads to a good approximation of the original dynamics when these time

Submitted to the editors on August 9, 2023. E. Zuazua has been funded by the Alexander von Humboldt-Professorship program, the ModConFlex Marie Curie Action, HORIZON-MSCA-2021-DN-01, the COST Action MAT-DYN-NET, the Transregio 154 Project “Mathematical Modelling, Simulation and Optimization Using the Example of Gas Networks” of the DFG, grants PID2020-112617GB-C22 and TED2021-131390B-I00 of MINECO (Spain), and by the Madrid Government – UAM Agreement for the Excellence of the University Research Staff in the context of the V PRICIT (Regional Programme of Research and Technological Innovation).

D. W. M. Veldman and E. Zuazua are with the Chair for Dynamics, Control, Machine Learning and Numerics – Alexander von Humboldt Professorship, Department of Mathematics, Friedrich-Alexander Universität Erlangen-Nürnberg, 91058, Erlangen, Bavaria, Germany (e-mail: daniel.wm.veldman@fau.de, enrique.zuazua@fau.de).

A. Borkowski is with the Department of Mathematics, Friedrich-Alexander Universität Erlangen-Nürnberg, 91058, Erlangen, Bavaria, Germany (e-mail: alexandra.borkowski@fau.de)

E. Zuazua is also with the Chair in Computational Mathematics, Fundación Deusto, Av. de las Universidades 24, 48007, Bilbao, Spain and Departamento de Matemáticas, Universidad Autónoma de Madrid, 28049, Madrid, Spain.

intervals are chosen sufficiently small, see, e.g., [4]. Recently, this idea has been extended to infinite-dimensional systems [5]. RBM-constrained OCPs have been analyzed in [6].

The RBM can be used to speed up the solution of the finite-horizon OCPs in MPC. The feedback nature of MPC also creates more robustness against the accumulating error in the RBM approximation (see, e.g., [6]). The effectiveness of this combination of MPC with RBM (RBM-MPC) for nonlinear interacting particle systems has been demonstrated in [7], but a rigorous stability and convergence analysis is still missing.

The RBM in RBM-MPC fulfills a similar role as the Reduced Order Models (ROM) in MPC based on ROMs. There has been research on stability guarantees for MPC based on ROMs in constrained linear systems, see, e.g., [8], [9]. The RBM is typically easier to apply than ROM techniques, but the analysis of RBM-MPC is nonetheless involved due to the stochasticity introduced by the RBM.

In this paper, we provide the first rigorous analysis of the RBM-MPC algorithm. Our analysis is limited to the unconstrained linear quadratic setting and thus extends the open-loop analysis from [6] to a closed-loop setting. The obtained error estimates demonstrate the influence of the different parameters in RBM-MPC on the expected performance, and the obtained convergence rates are validated in a numerical example.

The remainder of this paper is structured as follows. The RBM-MPC algorithm is presented in Section II. After the introduction of preliminary estimates and notation in Section III, the stability and convergence of RBM-MPC are proven in Sections IV and V, respectively. The convergence rates are validated in a numerical example in Section VI. Finally, conclusions and perspectives are presented in Section VII.

We will use the following notation. The (Euclidean) norm of a vector $\mathbf{x} \in \mathbb{R}^n$ is $|\mathbf{x}| = \sqrt{\mathbf{x}^\top \mathbf{x}}$. For a matrix $M \in \mathbb{R}^{n \times m}$, $\|M\| = \sup_{|\mathbf{x}|=1} |M\mathbf{x}|$. For symmetric $M \in \mathbb{R}^{n \times n}$, $M \succcurlyeq 0$ or $M \succ 0$ indicates that M is positive semi-definite or positive definite, respectively. For $M \succcurlyeq 0$, $|\mathbf{x}|_M = \sqrt{\mathbf{x}^\top M \mathbf{x}}$. In the tradition of e.g. [10], a matrix $M \in \mathbb{R}^{n \times n}$ is called *dissipative* when $\mathbf{x}^\top M \mathbf{x} \leq 0$ for all $\mathbf{x} \in \mathbb{R}^n$.

II. THE RBM-MPC ALGORITHM

The RBM-MPC algorithm analyzed in this paper is a way to approximate the control $\mathbf{u}_\infty^*(t)$ that minimizes

$$J_\infty(\mathbf{u}) = \int_0^\infty (|\mathbf{x}(t)|_Q^2 + |\mathbf{u}(t)|_W^2) dt, \quad (1)$$

subject to the dynamics

$$\dot{\mathbf{x}}(t) = A\mathbf{x}(t) + B\mathbf{u}(t), \quad \mathbf{x}(0) = \mathbf{x}_0, \quad (2)$$

where the state $\mathbf{x}(t)$ evolves in \mathbb{R}^n starting from the initial condition \mathbf{x}_0 , the control $\mathbf{u}(t)$ evolves in \mathbb{R}^m , $0 \preccurlyeq Q \in \mathbb{R}^{n \times n}$, $0 \prec W \in \mathbb{R}^{m \times m}$, $A \in \mathbb{R}^{n \times n}$, and $B \in \mathbb{R}^{n \times m}$. It is assumed that (A, B) is stabilizable and (A, Q) is detectable.

The OCP (1)–(2) can be approximated using MPC. In MPC, two parameters arise: the prediction horizon T and the shorter control horizon τ . Set $\tau_i := i\tau$ (with $i \in \mathbb{N}$) and let $\mathbf{u}_T^*(t; \mathbf{x}_{i-1}, \tau_{i-1})$ and $\mathbf{x}_T^*(t; \mathbf{x}_{i-1}, \tau_{i-1})$ denote the control and state trajectory that minimize

$$J_T(\mathbf{u}_T; \mathbf{x}_{i-1}, \tau_{i-1}) = |\mathbf{x}_T(\tau_{i-1} + T)|_F^2 + \int_{\tau_{i-1}}^{\tau_{i-1} + T} (|\mathbf{x}_T(t)|_Q^2 + |\mathbf{u}_T(t)|_W^2) dt, \quad (3)$$

where $F \succcurlyeq 0$ and $\mathbf{x}_T(t)$ fulfills for $t \in [\tau_{i-1}, \tau_{i-1} + T]$

$$\dot{\mathbf{x}}_T(t) = A\mathbf{x}_T(t) + B\mathbf{u}_T(t), \quad \mathbf{x}_T(\tau_{i-1}) = \mathbf{x}_{i-1}. \quad (4)$$

When n is large and A not sparse, finding $\mathbf{u}_T^*(t; \mathbf{x}_{i-1}, \tau_{i-1})$ and $\mathbf{x}_T^*(t; \mathbf{x}_{i-1}, \tau_{i-1})$ is computationally demanding. We therefore replace A by a randomized sparser matrix A_R .

The randomized matrix $A_R(\omega_i, t)$ is constructed as follows. First, A is written as the sum of *sparse* submatrices A_m

$$A = \sum_{m=1}^M A_m. \quad (5)$$

Next, the subsets of $\{1, 2, \dots, M\}$ are enumerated as S_1, S_2, \dots, S_{2^M} and a probability $p_\omega \in [0, 1]$ is assigned to each subset S_ω ($\omega \in \{1, 2, \dots, 2^M\}$) such that $\sum_\omega p_\omega = 1$.

The time interval $[0, T]$ is divided into K time intervals of equal length h . For each of the K time intervals, an element $\omega_{i,k} \in \{1, 2, \dots, 2^M\}$ of the vector ω_i is selected according to the probabilities p_ω . The matrix A_R is now defined as follows

$$A_R(\omega_i, t) = \sum_{m \in S_{\omega_{i,k}}} \frac{A_m}{\pi_m}, \quad t \in [(k-1)h, kh). \quad (6)$$

The scaling factors π_m are defined such that the expected value of $A_R(\omega_i, t)$ is equal to A . In particular, π_m denotes the probability of having the index m in the selected subset

$$\pi_m := \sum_{\omega \in \{\omega' \in \{1, 2, \dots, 2^M\} | m \in S_{\omega'}\}} p_\omega. \quad (7)$$

The definition of A_R thus requires that the probabilities p_ω are selected such that $\pi_m > 0$ for all $m \in \{1, 2, \dots, M\}$.

The dynamics generated by $A_R(\omega_i, t)$ is in expectation close to the dynamics generated by A for h sufficiently small (see [6]) and replacing A by $A_R(\omega_i, t)$ reduces the computational cost when $A_R(\omega_i, t)$ is much sparser than A . Consider therefore the control $\mathbf{u}_R^*(\omega_i, t; \mathbf{x}_{i-1}, \tau_{i-1})$ and state trajectory $\mathbf{x}_R^*(\omega_i, t; \mathbf{x}_{i-1}, \tau_{i-1})$ that minimize

$$J_R(\mathbf{u}_R; \omega_i, \mathbf{x}_{i-1}, \tau_{i-1}) = |\mathbf{x}_R(\omega_i, \tau_{i-1} + T)|_F^2 + \int_{\tau_{i-1}}^{\tau_{i-1} + T} (|\mathbf{x}_R(\omega_i, t)|_Q^2 + |\mathbf{u}_R(t)|_W^2) dt, \quad (8)$$

where $\mathbf{x}_R(t)$ fulfills for $t \in [\tau_{i-1}, \tau_{i-1} + T]$

$$\dot{\mathbf{x}}_R(\omega_i, t) = A_R(\omega_i, t - \tau_{i-1})\mathbf{x}_R(\omega_i, t) + B\mathbf{u}_R(t), \quad \mathbf{x}_R(\omega_i, \tau_{i-1}) = \mathbf{x}_{i-1}. \quad (9)$$

It has been proven in [6] that $\mathbf{u}_R^*(\omega_i, t; \mathbf{x}_{i-1}, \tau_{i-1})$ is (in expectation) close to $\mathbf{u}_T^*(t; \mathbf{x}_{i-1}, \tau_{i-1})$ for h small enough, see also Section III. Because $\mathbf{u}_R^*(\omega_i, t; \mathbf{x}_{i-1}, \tau_{i-1})$ is used to control the dynamics generated by A , consider also the solution $\mathbf{y}_R^*(\omega_i, t; \mathbf{x}_{i-1}, \tau_{i-1})$ of

$$\dot{\mathbf{y}}_R^*(\omega_i, t) = A\mathbf{y}_R^*(\omega_i, t) + B\mathbf{u}_R^*(\omega_i, t; \mathbf{x}_{i-1}, \tau_{i-1}), \quad \mathbf{y}_R^*(\omega_i, \tau_{i-1}) = \mathbf{x}_{i-1}. \quad (10)$$

where $\mathbf{y}_R^*(\omega_i, t)$ denotes $\mathbf{y}_R^*(\omega_i, t; \mathbf{x}_{i-1}, \tau_{i-1})$ for brevity.

The RBM-MPC algorithm now computes the control $\mathbf{u}_{R-M}(t)$ and state trajectory $\mathbf{x}_{R-M}(t)$ on $[0, \infty)$ as follows.

- 1) Initialize $\mathbf{x}_{R-M}(0) = \mathbf{x}_0$ and $i = 1$.
- 2) Select a random vector $\omega_i \in \{1, 2, \dots, 2^M\}^K$.
- 3) Compute $\mathbf{u}_R^*(\omega_i, t; \mathbf{x}_{R-M}(\tau_{i-1}), \tau_{i-1})$ and $\mathbf{y}_R^*(\omega_i, t; \mathbf{x}_{R-M}(\tau_{i-1}), \tau_{i-1})$ on $[\tau_{i-1}, \tau_{i-1} + T]$.
- 4) Set $\mathbf{u}_{R-M}(t) = \mathbf{u}_R^*(\omega_i, t; \mathbf{x}_{R-M}(\tau_{i-1}), \tau_{i-1})$ and $\mathbf{x}_{R-M}(t) = \mathbf{y}_R^*(t, \mathbf{x}_{R-M}(\tau_{i-1}), \tau_{i-1})$ on $[\tau_{i-1}, \tau_i]$.
- 5) Set $i = i + 1$ and go to Step 2.

Note that RBM-MPC reduces to standard MPC when $A_R(\omega_i, t) = A$ and that $\mathbf{x}_{R-M}(\tau_i)$ depends on the previously selected sequences ω_j with $j \leq i$, which are denoted by

$$\Omega_i := (\omega_1, \omega_2, \dots, \omega_i) \in \{1, 2, \dots, 2^M\}^{iK}. \quad (11)$$

The construction of the matrix $A_R(\omega_i, t)$ leaves freedom in the choice of the submatrices A_m , the probabilities p_ω , and the grid spacing h . As for the submatrices A_m , splittings of the form (5) are standard in operator-splitting methods, which are well-established in the numerical analysis, see, e.g., [11]. The specific choice of the A_m 's is often guided by physical insight. In many finite-dimensional examples, each A_m represents an interaction between two Degrees of Freedom (DOFs) so that $M \leq n(n-1)/2$, see, e.g., Section VI and [6, Section 4]. When there is no such physical insight, A can, for example, be divided into equal-sized blocks. Regarding the grid spacing h , note that the estimates in Theorems 1 and 2 below are proportional to $\sqrt{h \text{Var}[A_R]}$, where

$$\text{Var}[A_R] := \sum_{\omega=1}^{2^M} \left\| A - \sum_{m \in S_\omega} \frac{A_m}{\pi_m} \right\|^2 p_\omega. \quad (12)$$

Reducing $\text{Var}[A_R]$ thus enables us to use a larger step size h . Finally, note that assigning nonzero probabilities p_ω to larger subsets S_ω reduces $\text{Var}[A_R]$, but will also make $A_R(\omega_i, t)$ less sparse and thus potentially increases the computational cost, see [6, Section 2.3] for further discussions and examples of this trade-off.

Error estimates for the RBM, as in Section III and in Theorems 1 and 2, require a uniform quasi-dissipativity condition on A_R , i.e. there exists a $\mu_R \geq 0$ such that

$$\mathbf{x}^\top A_R(\omega_i, t) \mathbf{x} \leq \mu_R |\mathbf{x}|^2, \quad (13)$$

for all $\mathbf{x} \in \mathbb{R}^n$, $\omega_i \in \{1, 2, \dots, 2^M\}^K$, and $t \in [0, T]$.

Remark 1: Note that $\mu_R = 0$ when all A_m 's are dissipative. The latter condition can be achieved in many examples, see, e.g., Section VI and [6, Section 4].

Remark 2: Condition (13) readily extends to a setting in which the A_m 's are quasi-dissipative unbounded operators on

a Banach space, see, e.g. [10]. However, the appearance of the operator norm $\|\cdot\|$ in (12) is an indication that extending the RBM to such setting is not trivial, see, e.g. [5].

III. PRELIMINARY ESTIMATES

In the following, C denotes a constant depending only on A , B , Q , W , and F . The notation C_T indicates that the constant also depends on T . The constants C and C_T may vary from expression to expression, e.g. $(\|A\| + T)C_T \leq C_T$. Because we are interested in the limit $h\text{Var}[A_R] \rightarrow 0$, we will only consider the lowest power of $h\text{Var}[A_R]$ in our estimates.

The following lemma now directly follows from (13).

Lemma 1: The solution $\mathbf{x}_R(\boldsymbol{\omega}_i, t)$ of (9) satisfies for all $\tau_{i-1} \leq t \leq \tau_{i-1} + T$ and all $\boldsymbol{\omega}_i \in \{1, 2, \dots, 2^M\}^K$

$$|\mathbf{x}_R(\boldsymbol{\omega}_i, t)| \leq C_T e^{\mu_R(t-\tau_{i-1})} (|\mathbf{x}_{i-1}| + \|\mathbf{u}_R(\boldsymbol{\omega}_i)\|_{L^2(\tau_{i-1}, t; \mathbb{R}^q)}). \quad (14)$$

Proof: Differentiate $|\mathbf{x}_R(\boldsymbol{\omega}_i, t)|^2$ using (9), use (13), integrate from τ_{i-1} to t , apply Cauchy-Schwarz in $L^2(\tau_{i-1}, t; \mathbb{R}^q)$ and then Gronwall's lemma. ■

Our analysis will use Riccati theory. For the infinite-horizon OCP (1)–(2), let P_∞ denote the (unique) symmetric positive-definite solution of the Algebraic Riccati Equation (ARE)

$$A^\top P_\infty + P_\infty A - P_\infty B W^{-1} B^\top P_\infty + Q = 0. \quad (15)$$

It is then well-known that, see, e.g., [12, Section 5.1],

$$\mathbf{u}_\infty^*(t) = -W^{-1} B^\top P_\infty \mathbf{x}_\infty^*(t). \quad (16)$$

Therefore, $\mathbf{x}_\infty^*(t)$ follows the dynamics generated by

$$A_\infty = A - B W^{-1} B^\top P_\infty, \quad (17)$$

which is stable, i.e. there exist $M_\infty \geq 1$ and $\mu_\infty > 0$

$$\|e^{A_\infty t}\| \leq M_\infty e^{-\mu_\infty t}. \quad (18)$$

For the finite-horizon OCP (3)–(4), $t \in [0, T]$, let $P_T(t)$ solve the Riccati Differential Equation (RDE)

$$-\dot{P}_T(t) = A^\top P_T(t) + P_T(t) A - P_T(t) B W^{-1} B^\top P_T(t) + Q, \quad P_T(T) = F, \quad (19)$$

on $t \in [0, T]$. It is well-known that, see, e.g., [12, Section 5.2],

$$\mathbf{u}_T^*(t; \mathbf{x}_{i-1}, \tau_{i-1}) = -W^{-1} B^\top P_T(t - \tau_{i-1}) \mathbf{x}_T^*(t, \mathbf{x}_{i-1}, \tau_{i-1}). \quad (20)$$

For the randomized OCP (8)–(9), let $P_R(\boldsymbol{\omega}_i, t)$ solves the Randomized Riccati Differential Equation (RRDE) on $[0, T]$

$$\begin{aligned} \dot{P}_R(\boldsymbol{\omega}_i, t) &= A_R(\boldsymbol{\omega}_i, t)^\top P_R(\boldsymbol{\omega}_i, t) + P_R(\boldsymbol{\omega}_i, t) A_R(\boldsymbol{\omega}_i, t) \\ &\quad - P_R(\boldsymbol{\omega}_i, t) B W^{-1} B^\top P_R(\boldsymbol{\omega}_i, t) + Q, \quad P_R(\boldsymbol{\omega}_i, T) = F. \end{aligned} \quad (21)$$

Similarly as in (20), it holds that

$$\mathbf{u}_R^*(\boldsymbol{\omega}_i, t; \mathbf{x}_{i-1}, \tau_{i-1}) = -W^{-1} B^\top P_R(\boldsymbol{\omega}_i, t - \tau_{i-1}) \mathbf{x}_R^*(\boldsymbol{\omega}_i, t, \mathbf{x}_{i-1}, \tau_{i-1}). \quad (22)$$

The following lemma shows that $P_T(t) \rightarrow P_\infty$ for $T \rightarrow \infty$.

Lemma 2: If (A, B) is stabilizable, (A, Q) is detectable, and μ_∞ is as in (18), then for all $t \in [0, T]$

$$\|P_T(t) - P_\infty\| \leq C \|F - P_\infty\| e^{-2\mu_\infty(T-t)}. \quad (23)$$

Proof: See [13]. A shorter proof for the case that (A, B) is controllable and (A, Q) is observable is given in [14]. ■

Remark 3: Because $\|P_\infty\| \leq C$, Lemma 2 implies that $\|P_T(t)\| \leq C$.

Let V be a vector space. The expected value of a random variable $X : \{1, 2, \dots, 2^M\}^K \rightarrow V$ depending on $\boldsymbol{\omega}_i$ is

$$\mathbb{E}_i[X] = \sum_{\boldsymbol{\omega}_i \in \{1, 2, \dots, 2^M\}^K} X(\boldsymbol{\omega}_i) p(\boldsymbol{\omega}_i), \quad (24)$$

where $p(\boldsymbol{\omega}_i) = p_{\omega_{i,1}} p_{\omega_{i,2}} \dots p_{\omega_{i,K}}$. The expected value of a random variable $X : \{1, 2, \dots, 2^M\}^{iK} \rightarrow V$ is denoted by

$$\mathbb{E}[X] = \sum_{\boldsymbol{\omega}_1, \boldsymbol{\omega}_2, \dots, \boldsymbol{\omega}_i \in \{1, 2, \dots, 2^M\}^K} X(\boldsymbol{\omega}_1, \boldsymbol{\omega}_2, \dots, \boldsymbol{\omega}_i) \times p(\boldsymbol{\omega}_1) p(\boldsymbol{\omega}_2) \dots p(\boldsymbol{\omega}_i). \quad (25)$$

For the expected value of a random variable $X(\Omega_i)$ w.r.t. the last $\boldsymbol{\omega}_i$, we write $\mathbb{E}_i[X(\Omega_{i-1})]$ to indicate that the result depends on Ω_{i-1} . For random variables $X(\Omega_i)$ and $Y(\Omega_i)$,

$$\mathbb{E}[XY] \leq \sqrt{\mathbb{E}[X^2] \mathbb{E}[Y^2]}, \quad (26)$$

$$\sqrt{\mathbb{E}[(X+Y)^2]} \leq \sqrt{\mathbb{E}[X^2]} + \sqrt{\mathbb{E}[Y^2]}. \quad (27)$$

Similar expressions hold for the expectation \mathbb{E}_i .

For $0 \leq s \leq t \leq T$, let $S_R(\boldsymbol{\omega}_i, t, s)$ be the evolution operator generated by $A_R(\boldsymbol{\omega}_i, t)$, i.e. $S_R(\boldsymbol{\omega}_i, t, s) \mathbf{x} = \mathbf{x}(\boldsymbol{\omega}_i, t)$ where

$$\dot{\mathbf{x}}(\boldsymbol{\omega}_i, t) = A_R(\boldsymbol{\omega}_i, t) \mathbf{x}(\boldsymbol{\omega}_i, t), \quad \mathbf{x}(\boldsymbol{\omega}_i, s) = \mathbf{x}. \quad (28)$$

The following lemma from [6] then shows that $S_R(\boldsymbol{\omega}_i, t, s)$ is (in expectation) close to $e^{A(t-s)}$ when $h\text{Var}[A_R]$ is small.

Lemma 3: Let $\text{Var}[A_R]$ and μ_R be as in (12) and (13) and $0 \leq s \leq t \leq T$, then

$$\mathbb{E}_i[\|S_R(t, s) - e^{A(t-s)}\|^2] \leq C_T e^{2\mu_R(t-s)} h\text{Var}[A_R]. \quad (29)$$

Proof: See [6, Theorem 1 and Corollary 1]. ■

With Lemma 3, it is also possible to bound the difference between controlled state trajectories.

Lemma 4: Let $\mathbf{u}_R : \{1, 2, \dots, 2^M\}^K \times [\tau_{i-1}, \tau_{i-1} + T] \rightarrow \mathbb{R}^q$ be a random control and $\mathbf{x}_{i-1} : \{1, 2, \dots, 2^M\}^K \rightarrow \mathbb{R}^n$ a random initial condition. If $\mathbf{x}_R(\boldsymbol{\omega}_i, t)$ and $\mathbf{y}_R(\boldsymbol{\omega}_i, t)$ satisfy

$$\dot{\mathbf{x}}_R(\boldsymbol{\omega}_i, t) = A \mathbf{x}_R(\boldsymbol{\omega}_i, t) + B \mathbf{u}_R(\boldsymbol{\omega}_i, t), \quad (30)$$

$$\dot{\mathbf{y}}_R(\boldsymbol{\omega}_i, t) = A_R(\boldsymbol{\omega}_i, t - \tau_{i-1}) \mathbf{y}_R(\boldsymbol{\omega}_i, t) + B \mathbf{u}_R(\boldsymbol{\omega}_i, t), \quad (31)$$

$$\mathbf{x}_R(\boldsymbol{\omega}_i, \tau_{i-1}) = \mathbf{y}_R(\boldsymbol{\omega}_i, \tau_{i-1}) = \mathbf{x}_{i-1}(\boldsymbol{\omega}_i), \quad (32)$$

then

$$\mathbb{E}[\|\mathbf{y}_R(t; \mathbf{x}_i, \tau_i) - \mathbf{x}_R(t; \mathbf{x}_i, \tau_i)\|^2] \leq C_T e^{2\mu_R(t-\tau_i)} \times \quad (33)$$

$$h\text{Var}[A_R] \left(\max_{\boldsymbol{\omega}_i} |\mathbf{x}_{i-1}(\boldsymbol{\omega}_i)| + \max_{\boldsymbol{\omega}_i} \|\mathbf{u}_R(\boldsymbol{\omega}_i)\|_{L^2(\tau_{i-1}, t; \mathbb{R}^q)} \right)^2.$$

Proof: By a slight modification of [6, Theorem 2] in which the random initial condition was not considered. ■

We remark that although Riccati theory will be used in the analysis, the OCPs in Section II are typically more efficiently solved by a gradient-based algorithm, especially when n is large.

IV. STABILITY ANALYSIS

For the stability result in Theorem 1 at the end of this section, we first establish two lemmas. Consider $i \in \mathbb{N}$ and $t \in [\tau_{i-1}, \tau_i]$. Because $\mathbf{x}_{R-M}(\Omega_i, t)$ satisfies (10),

$$\dot{\mathbf{x}}_{R-M}(\Omega_i, t) = A_\infty \mathbf{x}_{R-M}(\Omega_i, t) + \mathbf{r}(\Omega_i, t), \quad (34)$$

with A_∞ as in (17) and

$$\begin{aligned} \mathbf{r}(\Omega_i, t) &= BW^{-1}B^\top P_\infty \mathbf{x}_{R-M}(\Omega_i, t) + B\mathbf{u}_R^*(\omega_i, t) \\ &= BW^{-1}B^\top (P_\infty - P_T(t - \tau_{i-1}))\mathbf{x}_{R-M}(\Omega_i, t) + \\ &\quad B \underbrace{(W^{-1}B^\top P_T(t - \tau_{i-1})\mathbf{x}_{R-M}(\Omega_i, t) + \mathbf{u}_R^*(\omega_i, t))}_{=: \mathbf{g}(\Omega_i, t)}, \end{aligned} \quad (35)$$

where $\mathbf{u}_R^*(\omega_i, t)$ denotes $\mathbf{u}_R^*(\omega_i, t; \mathbf{x}_{R-M}(\Omega_{i-1}, \tau_{i-1}), \tau_{i-1})$ for brevity. The first auxiliary lemma is now as follows.

Lemma 5: Let $P_R(\omega_i, t)$ and $P_T(t)$ satisfy (21) and (19), then, for $t \in [0, T]$,

$$\mathbb{E}_i[\|P_R(t) - P_T(t)\|] \leq C_T e^{2\mu_R T} \sqrt{h\text{Var}[A_R]}. \quad (36)$$

Proof: We will only proof (36) for $t = 0$. The result for $t > 0$ can be obtained similarly. By definition,

$$\begin{aligned} &\|P_R(\omega_i, 0) - P_T(0)\| \\ &= (\bar{\mathbf{x}}(\omega_i))^\top (P_R(\omega_i, 0) - P_T(0))\bar{\mathbf{x}}(\omega_i) \\ &= |J_R(\omega_i, \mathbf{u}_R^*(\omega_i); \bar{\mathbf{x}}(\omega_i), 0) - J_T(\mathbf{u}_T^*(\omega_i); \bar{\mathbf{x}}(\omega_i), 0)|, \end{aligned} \quad (37)$$

where $\bar{\mathbf{x}}(\omega_i) = \arg\max_{|\mathbf{x}|=1} |\mathbf{x}^\top (P_R(\omega_i, 0) - P_T(0))\mathbf{x}|$, $(\mathbf{u}_R^*(\omega_i), \mathbf{x}_R^*(\omega_i))$ and $(\mathbf{u}_T^*(\omega_i), \mathbf{x}_T^*(\omega_i))$ denote the control-state pairs that minimize $J_R(\omega_i, \cdot; \bar{\mathbf{x}}(\omega_i), 0)$ and $J_T(\cdot; \bar{\mathbf{x}}(\omega_i), 0)$, respectively. We also write $J_R(\omega_i, \cdot)$ and $J_T(\cdot)$ for $J_R(\omega_i, \cdot; \bar{\mathbf{x}}(\omega_i), 0)$ and $J_T(\cdot; \bar{\mathbf{x}}(\omega_i), 0)$, respectively.

Now introduce a random control $\mathbf{u}_{RT}(\omega_i, t)$ by setting it equal to $\mathbf{u}_T^*(\omega_i, t)$ when $J_T(\mathbf{u}_T^*(\omega_i)) \leq J_R(\omega_i, \mathbf{u}_R^*(\omega_i))$ and equal to $\mathbf{u}_R^*(\omega_i, t)$ otherwise and define $\mathbf{x}_{RT}(\omega_i, t)$ and $\mathbf{y}_{RT}(\omega_i, t)$ as the solutions of (30)–(32) on $[0, T]$ resulting from the control $\mathbf{u}_{RT}(\omega_i, t)$ and the IC $\bar{\mathbf{x}}(\omega_i)$.

When $J_T(\mathbf{u}_T^*(\omega_i)) \leq J_R(\omega_i, \mathbf{u}_R^*(\omega_i))$,

$$\begin{aligned} \|P_R(\omega_i, 0) - P_T(0)\| &= J_R(\omega_i, \mathbf{u}_R^*(\omega_i)) - J_T(\mathbf{u}_T^*(\omega_i)) \\ &\leq J_R(\omega_i, \mathbf{u}_{RT}(\omega_i)) - J_T(\mathbf{u}_{RT}(\omega_i)), \end{aligned} \quad (38)$$

because $\mathbf{u}_{RT}(\omega_i) = \mathbf{u}_T^*(\omega_i)$ and because $\mathbf{u}_R^*(\omega_i)$ minimizes $J_R(\omega_i, \cdot)$. Similarly, when $J_R(\omega_i, \mathbf{u}_R^*(\omega_i)) < J_T(\mathbf{u}_T^*(\omega_i))$

$$\begin{aligned} \|P_R(\omega_i, 0) - P_T(0)\| &= J_T(\mathbf{u}_T^*(\omega_i)) - J_R(\omega_i, \mathbf{u}_R^*(\omega_i)) \\ &\leq J_T(\mathbf{u}_{RT}(\omega_i)) - J_R(\omega_i, \mathbf{u}_{RT}(\omega_i)), \end{aligned} \quad (39)$$

because $\mathbf{u}_{RT}(\omega_i) = \mathbf{u}_R^*(\omega_i)$ and $\mathbf{u}_T^*(\omega_i)$ minimizes $J_T(\cdot)$. Combining (38) and (39) thus shows that

$$\begin{aligned} \|P_R(\omega_i, 0) - P_T(0)\| &\leq |J_R(\omega_i, \mathbf{u}_{RT}(\omega_i)) - J_T(\mathbf{u}_{RT}(\omega_i))| \\ &\leq \|\mathbf{y}_{RT}(\omega_i, T)\|_F^2 - \|\mathbf{x}_{RT}(\omega_i, T)\|_F^2 \\ &\quad + \langle \mathbf{y}_{RT}(\omega_i), Q\mathbf{y}_{RT}(\omega_i) \rangle_{L^2} - \langle \mathbf{x}_{RT}(\omega_i), Q\mathbf{x}_{RT}(\omega_i) \rangle_{L^2} \\ &\leq |\langle 2\mathbf{x}_{RT}(\omega_i, T) + \mathbf{e}_{RT}(\omega_i, T), F\mathbf{e}_{RT}(\omega_i, T) \rangle| \\ &\quad + |\langle 2\mathbf{x}_{RT}(\omega_i) + \mathbf{e}_{RT}(\omega_i), Q\mathbf{e}_{RT}(\omega_i) \rangle_{L^2}| \\ &\leq 2\|\mathbf{x}_{RT}(\omega_i, T)\|_F \|\mathbf{e}_{RT}(\omega_i, T)\|_F + \|\mathbf{e}_{RT}(\omega_i, T)\|_F^2 \\ &\quad + 2\sqrt{\langle \mathbf{x}_{RT}(\omega_i), Q\mathbf{x}_{RT}(\omega_i) \rangle_{L^2} \langle \mathbf{e}_{RT}(\omega_i), Q\mathbf{e}_{RT}(\omega_i) \rangle_{L^2}} \\ &\quad + \langle \mathbf{e}_{RT}(\omega_i), Q\mathbf{e}_{RT}(\omega_i) \rangle_{L^2}, \end{aligned} \quad (40)$$

where $\langle \cdot, \cdot \rangle_{L^2}$ denotes the L^2 -inner product on $[0, T]$ and

$$\mathbf{e}_{RT}(\omega_i, t) = \mathbf{y}_{RT}(\omega_i, t) - \mathbf{x}_{RT}(\omega_i, t). \quad (41)$$

Furthermore, when $J_T(\mathbf{u}_T^*(\omega_i)) \leq J_R(\omega_i, \mathbf{u}_R^*(\omega_i))$,

$$\begin{aligned} \|\mathbf{x}_{RT}(\omega_i, T)\|_F^2 + \langle \mathbf{x}_{RT}(\omega_i), Q\mathbf{x}_{RT}(\omega_i) \rangle_{L^2} + \alpha \|\mathbf{u}_{RT}(\omega_i)\|_{L^2}^2 \\ \leq J_T(\mathbf{u}_T^*(\omega_i)) = \|\bar{\mathbf{x}}(\omega_i)\|_{P_T(0)}^2 \leq C \|\bar{\mathbf{x}}(\omega_i)\|^2, \end{aligned} \quad (42)$$

where $\alpha > 0$ is the smallest eigenvalue of W and it has been used that $\|P_T(t)\| \leq C$, see Remark 3. When $J_R(\omega_i, \mathbf{u}_R^*(\omega_i)) < J_T(\mathbf{u}_T^*(\omega_i))$

$$\begin{aligned} \|\mathbf{x}_{RT}(\omega_i, T)\|_F^2 + \langle \mathbf{x}_{RT}(\omega_i), Q\mathbf{x}_{RT}(\omega_i) \rangle_{L^2} + \alpha \|\mathbf{u}_{RT}(\omega_i)\|_{L^2}^2 \\ \leq J_R(\omega_i, \mathbf{u}_R^*(\omega_i)) \leq J_T(\mathbf{u}_T^*(\omega_i)) \leq C \|\bar{\mathbf{x}}(\omega_i)\|^2. \end{aligned} \quad (43)$$

Because $\|\bar{\mathbf{x}}(\omega_i)\| = 1$ and because (42) and (43) show that $\|\mathbf{x}_{RT}(\omega_i, T)\|_F \leq C$ and $\langle \mathbf{x}_{RT}(\omega_i), Q\mathbf{x}_{RT}(\omega_i) \rangle_{L^2} \leq C$, taking the expectation in (40) thus shows that

$$\begin{aligned} \mathbb{E}_i[\|P_R(0) - P_T(0)\|] &\leq C\mathbb{E}_i[\|\mathbf{e}_{RT}(T)\|] + C\mathbb{E}_i[\|\mathbf{e}_{RT}(T)\|^2] \\ &\quad + C\mathbb{E}_i[\|\mathbf{e}_{RT}\|_{L^2}] + C\mathbb{E}_i[\|\mathbf{e}_{RT}\|_{L^2}^2]. \end{aligned} \quad (44)$$

Because $\|\bar{\mathbf{x}}(\omega_i)\| = 1$ and because (42) and (43) show that $\|\mathbf{u}_{RT}(\omega_i)\|_{L^2} \leq C$, applying Lemma 4 shows that

$$\mathbb{E}_i[\|\mathbf{e}_{RT}(t)\|] \leq C_T e^{2\mu_R T} h\text{Var}[A_R], \quad (45)$$

which also implies that $\mathbb{E}_i[\|\mathbf{e}_{RT}\|_{L^2}^2] \leq C_T e^{2\mu_R T} h\text{Var}[A_R]$. Because $\mathbb{E}_i[X] \leq \sqrt{\mathbb{E}_i[X^2]}$, (44) now shows that

$$\begin{aligned} \mathbb{E}_i[\|P_R(0) - P_T(0)\|] \\ \leq C_T e^{2\mu_R T} \left(\sqrt{h\text{Var}[A_R]} + h\text{Var}[A_R] \right). \end{aligned} \quad (46)$$

As we are interested in the limit $h\text{Var}[A_R] \rightarrow 0$, we assume that $h\text{Var}[A_R] \leq C$ (cf. the first paragraph of Section III) and (36) follows because $h\text{Var}[A_R] \leq C\sqrt{h\text{Var}[A_R]}$. ■

With this result, $\mathbb{E}_i[\|\mathbf{g}(\Omega_{i-1}, t)\|]$ can be bounded as follows.

Lemma 6: Let $\mathbf{g}(\Omega_i, t)$ be as in (35), then

$$\begin{aligned} \mathbb{E}_i[\|\mathbf{g}(\Omega_{i-1}, t)\|] \\ \leq C_T e^{\mu_R(2T+\tau)} \sqrt{h\text{Var}[A_R]} \|\mathbf{x}_{R-M}(\Omega_{i-1}, \tau_{i-1})\|. \end{aligned} \quad (47)$$

Proof: By using (22), the expression for $\mathbf{g}(\Omega_i, t)$ in (35) can be rewritten as

$$\begin{aligned} \mathbf{g}(\Omega_i, t) &= W^{-1}B^\top P_T(t - \tau_{i-1})(\mathbf{x}_{R-M}(\Omega_i, t) - \mathbf{x}_R^*(\omega_i, t)) \\ &\quad + W^{-1}B^\top (P_T(t - \tau_{i-1}) - P_R(\omega_{i-1}, t - \tau_{i-1}))\mathbf{x}_R^*(\omega_i, t). \end{aligned}$$

Taking the norm and expectation w.r.t. ω_i yields

$$\begin{aligned} \mathbb{E}_i[\|\mathbf{g}(\Omega_{i-1}, t)\|] &\leq C\mathbb{E}_i[\|\mathbf{x}_{R-M}(\Omega_{i-1}, t) - \mathbf{x}_R^*(t)\|] \\ &\quad + C\mathbb{E}_i[\|P_T(t - \tau_i) - P_R(t - \tau_i)\|] \max_{\omega_i} \|\mathbf{x}_R^*(\omega_i, t)\|. \end{aligned} \quad (48)$$

Lemma 5 gives a bound for $\mathbb{E}_i[\|P_T(t - \tau_i) - P_R(t - \tau_i)\|]$.

For $\mathbb{E}_i[\|\mathbf{x}_{R-M}(\Omega_{i-1}, t) - \mathbf{x}_R^*(t)\|]$, apply Lemma 4 with $\mathbf{u}_R(\omega_i, t) = \mathbf{u}_R^*(\omega_i, t; \mathbf{x}_{R-M}(\Omega_{i-1}, \tau_i), \tau_i)$ and the initial condition $\mathbf{x}_i(\omega_i) = \mathbf{x}_{R-M}(\Omega_{i-1}, \tau_i)$. This makes

$$\begin{aligned} \mathbf{y}_R(\omega_i, t) &= \mathbf{x}_R^*(\omega_i, t; \mathbf{x}_{R-M}(\Omega_{i-1}, \tau_i), \tau_i), \\ \mathbf{x}_R(\omega_i, t) &= \mathbf{y}_R^*(\omega_i, t; \mathbf{x}_{R-M}(\Omega_{i-1}, \tau_i), \tau_i) = \mathbf{x}_{R-M}(\Omega_i, t). \end{aligned}$$

The initial condition $\mathbf{x}_{R-M}(\Omega_{i-1}, \tau_{i-1})$ does not depend on ω_i . Let α again denote the smallest eigenvalue of W , then

$$\begin{aligned} \alpha |\mathbf{u}_R^*(\omega_i)|_{L^2}^2 &\leq J_R(\omega_i, \mathbf{u}_R^*(\omega_i); \mathbf{x}_{R-M}(\Omega_{i-1}, \tau_i), \tau_i) \\ &\leq J_R(\omega_i, 0; \mathbf{x}_{R-M}(\Omega_{i-1}, \tau_i), \tau_i) \\ &\leq C \|\mathbf{x}_R(\omega_i; \mathbf{x}_{R-M}(\Omega_{i-1}, \tau_i), \tau_i)\|_{L^2(\tau_{i-1}, \tau_{i-1}+T; \mathbb{R}^q)}^2 \\ &\leq C_T e^{2\mu_R T} \|\mathbf{x}_{R-M}(\Omega_{i-1}, \tau_{i-1})\|^2, \end{aligned} \quad (49)$$

where $\mathbf{x}_R(\omega_i, t; \mathbf{x}_i, \tau_i)$ satisfies (9) with $\mathbf{u}_R(t) = 0$ and $\mathbf{x}_{i-1} = \mathbf{x}_{R-M}(\Omega_{i-1}, \tau_{i-1})$ and the last inequality follows from Lemma 1. Lemma 4 now shows that

$$\begin{aligned} \mathbb{E}_i[\|\mathbf{x}_{R-M}(\Omega_{i-1}, t) - \mathbf{x}_R^*(t)\|] &\leq \sqrt{\mathbb{E}_i[\|\mathbf{x}_{R-M}(\Omega_{i-1}, t) - \mathbf{x}_R^*(t)\|^2]} \\ &\leq C_T e^{\mu_R T} \sqrt{h \text{Var}[A_R]} e^{\mu_R T} \|\mathbf{x}_{R-M}(\Omega_{i-1}, \tau_{i-1})\|. \end{aligned} \quad (50)$$

To bound $\|\mathbf{x}_R^*(\omega_i, t)\|$, note that $\mathbf{x}_R^*(\omega_i, t)$ satisfies (9) with $\mathbf{u}_R(\omega_i, t) = \mathbf{u}_R^*(\omega_i, t)$ and $\mathbf{x}_{i-1} = \mathbf{x}_{R-M}(\Omega_{i-1}, \tau_{i-1})$. Inserting (49) into (14) thus shows that for $t \in [\tau_{i-1}, \tau_i]$

$$\|\mathbf{x}_R^*(\omega_i, t)\| \leq C_T e^{\mu_R(T+\tau)} \|\mathbf{x}_{R-M}(\Omega_{i-1}, \tau_{i-1})\|. \quad (51)$$

Inserting (50), (36), and (51) into (48) completes the proof. ■

We are now ready to prove the main stability result.

Theorem 1: If (A, B) is stabilizable, (A, Q) is detectable, and M_∞ and μ_∞ are as in (18), then

$$\mathbb{E}[\|\mathbf{x}_{R-M}(t)\|] \leq M_\infty e^{-\mu_{R-M} t} \|\mathbf{x}_0\|, \quad (52)$$

where

$$\begin{aligned} \mu_{R-M} &= \mu_\infty - C \|F - P_\infty\| e^{-2\mu_\infty(T-\tau)} \\ &\quad - C_T e^{\mu_R(2T+\tau)} e^{\mu_\infty \tau} \sqrt{h \text{Var}[A_R]}. \end{aligned} \quad (53)$$

Proof: Applying the variation of constants formula to (34), taking the norm and the expectation yields

$$\begin{aligned} \mathbb{E}[\|\mathbf{x}_{R-M}(t)\|] &\leq M_\infty e^{-\mu_\infty t} \|\mathbf{x}_0\| \\ &\quad + M_\infty \int_0^t e^{-\mu_\infty(t-s)} \mathbb{E}[\|\mathbf{r}(s)\|] \, ds, \end{aligned} \quad (54)$$

where (18) has been used. Taking the norm and the expectation (first w.r.t. $\omega_{\lfloor s/\tau \rfloor + 1}$ and then w.r.t. to the other ω_j 's) in (35) using Lemmas 2 and 6, it follows that

$$\mathbb{E}[\|\mathbf{r}(s)\|] \leq C_1 \mathbb{E}[\|\mathbf{x}_{R-M}(s)\|] + C_2 \mathbb{E}[\|\mathbf{x}_{R-M}(\tau_{\lfloor s/\tau \rfloor})\|], \quad (55)$$

where we have introduced $C_1 = C \|F - P_\infty\| e^{-2\mu_\infty(T-\tau)}$ and $C_2 = C_T e^{\mu_R(2T+\tau)} \sqrt{h \text{Var}[A_R]}$. By inserting (55) into (54) and writing $f(t) = \mathbb{E}[\|\mathbf{x}_{R-M}(t)\|]$, we obtain

$$\begin{aligned} f(t) &\leq M_\infty e^{-\mu_\infty t} \|\mathbf{x}_0\| \\ &\quad + \int_0^t e^{-\mu_\infty(t-s)} (C_1 f(s) + C_2 f(\tau_{\lfloor s/\tau \rfloor})) \, ds. \end{aligned} \quad (56)$$

Setting $\hat{f}(t) = e^{\mu_\infty t} f(t)$, it follows that $\hat{f}(t) \leq \hat{F}(t)$ where

$$\hat{F}(t) = M_\infty \|\mathbf{x}_0\| + \int_0^t (C_1 \hat{f}(s) + C_2 e^{\mu_\infty \tau} \hat{f}(\tau_{\lfloor s/\tau \rfloor})) \, ds.$$

Because $\hat{F}(t)$ is monotonically increasing and $\hat{f}(t) \leq \hat{F}(t)$,

$$\hat{F}(t) \leq M_\infty \|\mathbf{x}_0\| + (C_1 + C_2 e^{\mu_\infty \tau}) \int_0^t \hat{F}(s) \, ds. \quad (57)$$

By Gronwall's lemma, we thus obtain that

$$e^{\mu_\infty t} f(t) = \hat{f}(t) \leq \hat{F}(t) \leq M_\infty \|\mathbf{x}_0\| e^{(C_1 + C_2 e^{\mu_\infty \tau})t}, \quad (58)$$

and the result follows. ■

Remark 4: Note that $\mu_{R-M} > 0$ will be positive for $h \text{Var}[A_R]$ and $\|F - P_\infty\| e^{-2\mu_\infty(T-\tau)}$ sufficiently small.

Remark 5: When $\mu_{R-M} > 0$, the RBM-MPC strategy is stabilizing with probability 1. To see this, note that Markov's inequality [15] and Theorem 1 imply that for any $\varepsilon > 0$

$$\mathbb{P}[\|\mathbf{x}_{R-M}(t)\| \geq \varepsilon] \leq \frac{\mathbb{E}[\|\mathbf{x}_{R-M}(t)\|]}{\varepsilon} \leq \frac{M_\infty e^{-t\mu_{R-M}} \|\mathbf{x}_0\|}{\varepsilon}.$$

Because $\mu_{R-M} > 0$, the probability that $\mathbf{x}_{R-M}(t)$ is outside any ε -neighborhood of the origin approaches zero for $t \rightarrow \infty$.

V. CONVERGENCE

We first consider the convergence of MPC. Note that $\mathbf{x}_M(t)$ follows the dynamics generated by the τ -periodic matrix

$$A_\tau(t) = A - BW^{-1}B^\top P_T(t \bmod \tau). \quad (59)$$

We then have the following lemma.

Lemma 7: If (A, B) is stabilizable, (A, Q) is detectable and M_∞ and μ_∞ are as in (18), then for all $0 \leq s \leq t$

$$\|e^{\int_s^t A_\tau(\sigma) \, d\sigma}\| \leq M_\infty e^{-\mu_M t}, \quad (60)$$

where

$$\mu_M = \mu_\infty - C \|F - P_\infty\| e^{-2\mu_\infty(T-\tau)}. \quad (61)$$

Furthermore, if $\mu_M > 0$, then

$$\begin{aligned} \|\mathbf{x}_M(t) - \mathbf{x}_\infty^*(t)\| + \|\mathbf{u}_M(t) - \mathbf{u}_\infty^*(t)\| &\leq C \|F - P_\infty\| e^{-2\mu_\infty(T-\tau)} \|\mathbf{x}_0\|. \end{aligned} \quad (62)$$

Remark 6: Lemma 7 shows that the dynamics generated by $A_\tau(t)$ is stable for $T - \tau$ sufficiently large or $\|F - P_\infty\|$ sufficiently small and that $(\mathbf{x}_M(t), \mathbf{u}_M(t)) \rightarrow (\mathbf{x}_\infty^*(t), \mathbf{u}_\infty^*(t))$ for $T - \tau \rightarrow \infty$ or $\|F - P_\infty\| \rightarrow 0$.

Proof: Let $\mathbf{x}(t)$ denote the solution to $\dot{\mathbf{x}}(t) = A_\tau(t)\mathbf{x}(t)$ with initial condition $\mathbf{x}(s) = \mathbf{x}_s$. By (17),

$$\dot{\mathbf{x}}(t) = (A_\infty + BW^{-1}B^\top(P_\infty - P_T(t \bmod \tau))) \mathbf{x}(t). \quad (63)$$

The variation of constants formula thus shows that

$$\begin{aligned} \mathbf{x}(t) &= e^{A_\infty(t-s)} \mathbf{x}_s \\ &\quad + \int_s^t e^{A_\infty(t-\sigma)} BW^{-1}B^\top (P_\infty - P_T(\sigma \bmod \tau)) \mathbf{x}(\sigma) \, d\sigma. \end{aligned}$$

Taking norms using (18) and Lemma 2, it follows that

$$\begin{aligned} \|\mathbf{x}(t)\| &= M_\infty e^{-\mu_\infty(t-s)} \|\mathbf{x}_s\| \\ &\quad + C \|F - P_\infty\| e^{-2\mu_\infty(T-\tau)} \int_s^t \|\mathbf{x}(\sigma)\| \, d\sigma. \end{aligned} \quad (64)$$

Applying Gronwall's lemma and noting that the initial condition \mathbf{x}_s is arbitrary now yields (60).

For the bound on $\mathbf{e}_M(t) := \mathbf{x}_M(t) - \mathbf{x}_\infty^*(t)$ in (62), note that $\dot{\mathbf{x}}_\infty^*(t) = A_\infty \mathbf{x}_\infty^*(t)$ and that $\mathbf{x}_M(t)$ satisfies (63), so that $\dot{\mathbf{e}}_M(t) = A_\infty \mathbf{e}_M(t) - BW^{-1}B^\top (P_T(t \bmod \tau) - P_\infty) \mathbf{x}_M(t)$.

Applying the variation of constants formula and taking the norm using (18), Lemma 2, and that $|\mathbf{x}_M(t)| \leq M_\infty |\mathbf{x}_0| \leq C|\mathbf{x}_0|$ when $\mu_M \geq 0$ by (60), it follows that

$$|e_M(t)| \leq C \|F - P_\infty\| e^{2\mu_\infty(T-\tau)} \int_0^t e^{\mu_\infty(t-s)} ds |\mathbf{x}_0|. \quad (65)$$

The bound on $e_M(t)$ follows because the remaining integral is bounded by $1/\mu_\infty \leq C$. For $\mathbf{u}_M(t) - \mathbf{u}_\infty(t)$, note that (20) implies that

$$\mathbf{u}_M(t) = -W^{-1}B^\top P_T(t \bmod \tau) \mathbf{x}_M(t), \quad (66)$$

so that subtracting (16) shows that

$$\mathbf{u}_M(t) - \mathbf{u}_\infty(t) = W^{-1}B^\top (P_\infty - P_T(t \bmod \tau)) \mathbf{x}_M(t) - W^{-1}B^\top P_\infty e_M(t). \quad (67)$$

Using Lemma 2 and that $|\mathbf{x}_M(t)| \leq M_\infty |\mathbf{x}_0| \leq C|\mathbf{x}_0|$ for the first term, and the previously derived bound for $|e_M(t)|$ for the second, the result follows. ■

We are now ready to prove the convergence of the RBM-MPC algorithm.

Theorem 2: If (A, B) is stabilizable, (A, Q) is detectable, and μ_{R-M} in (53) is positive, then

$$\begin{aligned} \mathbb{E}[|\mathbf{x}_{R-M}(t) - \mathbf{x}_M(t)|] + \mathbb{E}[|\mathbf{u}_{R-M}(t) - \mathbf{u}_M(t)|] \\ \leq \frac{C_T}{\mu_M} e^{\mu_R(2T+\tau)} \sqrt{h \text{Var}[A_R]} |\mathbf{x}_0|. \end{aligned} \quad (68)$$

Proof: Consider $i \in \mathbb{N}$ and $t \in [\tau_{i-1}, \tau_i)$. For the bound on $e_{R-M}(\Omega_i, t) = \mathbf{x}_{R-M}(\Omega_i, t) - \mathbf{x}_M(t)$, note that $\mathbf{x}_M(t)$ satisfies (63), so that (35) into (34) and subtracting (63) yields

$$\dot{e}_{R-M}(\Omega_i, t) = A_\tau(t) e_{R-M}(\Omega_i, t) + Bg(\Omega_i, t), \quad (69)$$

and $e_{R-M}(\Omega_i, 0) = 0$. Applying the variation of constants formula, taking the norm and the expectation thus shows that

$$\mathbb{E}[|e_{R-M}(t)|] = C \int_0^t \left\| e^{\int_s^t A_\tau(\sigma) d\sigma} \right\| \mathbb{E}[|g(s)|] ds. \quad (70)$$

By Lemma 6, it follows that

$$\begin{aligned} \mathbb{E}[|g(s)|] &\leq C_T e^{\mu_R(2T+\tau)} \sqrt{h \text{Var}[A_R]} \mathbb{E}[|\mathbf{x}_{R-M}(\tau_{\lfloor s/\tau \rfloor})|] \\ &\leq C_T e^{\mu_R(2T+\tau)} \sqrt{h \text{Var}[A_R]} |\mathbf{x}_0| \end{aligned} \quad (71)$$

where it has been used that $\mathbb{E}[|\mathbf{x}_{R-M}(t)|] \leq M_\infty |\mathbf{x}_0| \leq C|\mathbf{x}_0|$ by Theorem 1 because $\mu_{R-M} \geq 0$. Using (60) and (71) in (70), the bound for $e_{R-M}(\Omega_i, t)$ follows because the integral of $e^{-\mu_M(t-s)}$ is bounded by $1/\mu_M$.

To bound $\mathbf{u}_{R-M}(\Omega_i, t) - \mathbf{u}_M(t)$, note that for $t \in [\tau_{i-1}, \tau_i)$

$$\mathbf{u}_{R-M}(\Omega_i, t) = \mathbf{u}_R^*(\omega_i, t; \mathbf{x}_{R-M}(\Omega_{i-1}, \tau_{i-1}), \tau_{i-1}). \quad (72)$$

Subtracting (66) using the definition of $g(\Omega_i, t)$ in (35) yields

$$\begin{aligned} \mathbf{u}_{R-M}(\Omega_i, t) - \mathbf{u}_M(t) = \\ g(\Omega_i, t) - W^{-1}B^\top P_T(t \bmod \tau) e_{R-M}(\Omega_i, t). \end{aligned} \quad (73)$$

The bound now follows after taking the norm and the expected value, and then using Lemma 6 to bound $\mathbb{E}[|g(t)|]$ and the previously derived estimate for $\mathbb{E}[|e_{R-M}(t)|]$. ■

Remark 7: Combining Theorem 2 and (62), one obtains estimates for $\mathbb{E}[|\mathbf{x}_{R-M}(t) - \mathbf{x}_\infty^*(t)|] + \mathbb{E}[|\mathbf{u}_{R-M}(t) - \mathbf{u}_\infty^*(t)|]$.

The estimates also indicate a natural approach to tuning the parameters in RBM-MPC. First, $T - \tau$ should be chosen such that the MPC strategy is stabilizing with sufficient margin, i.e. such that $C\|F - P_\infty\|e^{2\mu_\infty(T-\tau)} \ll \mu_\infty$. After that, h can be chosen such that $\mu_{R-M} > 0$ and such that RBM-MPC leads to a sufficiently good approximation of MPC.

VI. NUMERICAL EXAMPLE

We consider a problem of the form (1)–(2) with $n \in \{11, 101, 1001\}$ states and $m = 1$ input, $A \in \mathbb{R}^{n \times n}$ is

$$A = (n-1)^2 \begin{bmatrix} -2 & 1 & 0 & \cdots & 0 & 1 \\ 1 & -2 & 1 & & 0 & 0 \\ 0 & 1 & -2 & & 0 & 0 \\ \vdots & & & \ddots & & \\ 0 & 0 & 0 & & -2 & 1 \\ 1 & 0 & 0 & & 1 & -2 \end{bmatrix}, \quad (74)$$

the first $(n-1)/10$ entries of $B \in \mathbb{R}^{n \times 1}$ are 1 and the others are zero, $Q = I_n/(n-1)$, and $R = 1$, where I_n denotes the $n \times n$ identity matrix. The matrix A in (74) could for example be obtained as a spatial discretization of a heat equation on a circle. The time interval $[0, \infty)$ is truncated to $[0, 200]$ and discretized by the Crank-Nicholson scheme with a step size $\Delta t = 1$. Note that every time step has a cost of $O(n^3)$, because the matrix $A - \frac{\Delta t}{2} I_n$ is not tridiagonal. The OCPs are solved by a steepest descent algorithm, in which the gradients are computed using the adjoint state, see [16], and the stepsize minimizes the functional in the direction of the gradient. The algorithm is stopped when the relative change in the control is below 10^{-5} or after 1000 iterations.

To construct the randomized matrix $A_R(\omega_i, t)$, note that A can be written as the sum of $M = n$ interconnection matrices as in (5), where the first $n-1$ interconnection matrices A_m are zero except for a diagonal block of the form

$$(n-1)^2 \begin{bmatrix} -1 & 1 \\ 1 & -1 \end{bmatrix}, \quad (75)$$

and the last interconnection matrix has only nonzero entries in its four corners. The sum of the first $n-1$ interconnection matrices leads to a tridiagonal matrix, which reduces the computational cost for each time step to $O(n)$, see, e.g., [11, Section 2.1.1]. In fact, the symmetry of the problem implies that omitting *any* one of the n submatrices A_m reduces the computational cost for one time step to $O(n)$. A probability $1/n$ is assigned to each subset of $\{1, 2, \dots, n\}$ of size $n-1$. The probabilities π_m in (7) are thus

$$\pi_m = \frac{n-1}{n}. \quad (76)$$

The grid spacing h is chosen as small as possible, so $h = \Delta t$. All A_m are dissipative, so $\mu_R = 0$ by Remark 1.

Figure 1a compares 20 realizations of the RBM-MPC control $u_{R-M}(\Omega_i, t)$ to the MPC control $u_M(t)$ and the infinite horizon control $u_\infty^*(t)$ for $n = 100$ spatial grid points. As can be seen, $u_\infty^*(t)$ is smooth, $u_M(t)$ jumps when t is a multiple of $\tau = 10$, and the realizations of $u_{R-M}(\Omega_i, t)$ contain high-frequency oscillations related to the grid spacing $\Delta t = h = 1$. Figure 1b shows that despite the relatively large deviations

TABLE I

RUNNING TIMES FOR A VARYING NUMBER OF SPATIAL GRID POINTS n
($h = 1$, $T = 15$, $\tau = 10$)

Running times [s]	$n = 10$	$n = 100$	$n = 1000$
Optimal Control	12.9 (± 1.35)	32.7 (± 1.53)	218.5 (± 4.36)
MPC	4.6 (± 0.44)	11.0 (± 0.66)	70.5 (± 4.51)
RBM-MPC	2.0 (± 0.23)	3.6 (± 0.71)	14.1 (± 1.33)

TABLE II

ERRORS FOR A VARYING NUMBER OF SPATIAL GRID POINTS n
($h = 1$, $T = 15$, $\tau = 10$)

Relative errors [-]	$n = 10$	$n = 100$	$n = 1000$
$ u_{R-M} - u_{\infty}^* _{L^2}$	0.76 (± 0.28)	0.59 (± 0.23)	0.53 (± 0.11)
$ u_{R-M} - u_M _{L^2}$	0.63 (± 0.30)	0.41 (± 0.27)	0.33 (± 0.16)
$ u_M - u_{\infty}^* _{L^2}$	0.41 (± 0.00)	0.37 (± 0.00)	0.39 (± 0.00)
$\ \mathbf{x}_{R-M} - \mathbf{x}_{\infty}^*\ _{L^{\infty}}$	0.35 (± 0.09)	0.28 (± 0.08)	0.25 (± 0.04)
$\ \mathbf{x}_{R-M} - \mathbf{x}_M\ _{L^{\infty}}$	0.17 (± 0.08)	0.11 (± 0.07)	0.08 (± 0.04)
$\ \mathbf{x}_M - \mathbf{x}_{\infty}^*\ _{L^{\infty}}$	0.24 (± 0.00)	0.22 (± 0.00)	0.22 (± 0.00)

of $u_{R-M}(\Omega_i, t)$ from $u_M(t)$, $|x_{R-M}(\Omega_i, t)|$ is very close to $|x_M(t)|$ for all 20 considered realizations Ω_i . RBM-MPC thus leads to almost the same decay rate as the MPC here. Note that $T = 15$ is not much larger than $\tau = 10$, but the simulations indicate that MPC and RBM-MPC are stabilizing.

Table I shows that the running times for RBM-MPC are smaller than those for MPC, which are again smaller than those for solving the OCP on $[0, 200]$ directly. The numbers between round brackets in Table I indicate the estimated standard deviation of the running times based on 20 runs. For $n = 100$, MPC is almost 3 times faster than a classical optimal control approach, and RBM-MPC is again almost 3 times faster than MPC. For $n = 1000$, MPC is still approximately 3 times faster than solving the OCP directly, but RBM-MPC is 5 times faster than MPC. Note that the relative speed up of RBM-MPC compared to MPC is not of $O(n^2)$ as the theoretical estimates predict because it also includes overheads and because solving the RBM-constrained OCP sometimes requires a few more iterations than the original OCP.

These observations are particularly interesting because Table II shows that the errors do not increase significantly when n is increased. The numbers between round brackets in Table II indicate the estimated standard deviation based on 20 realizations of Ω_i . Here, $\|\mathbf{x}\|_{L^{\infty}} := \max_t \sqrt{(\mathbf{x}(t))^{\top} \mathbf{x}(t)}/n$.

The convergence rates from Lemma 7 and Theorem 2 are validated in Figure 2 and 3. Figures 2a and 3a show that $\|\mathbf{x}_{R-M}(\Omega_i) - \mathbf{x}_M\|_{L^{\infty}}$ and $|u_{R-M}(\Omega_i) - u_M|_{L^2}$ decay as \sqrt{h} for $h \rightarrow 0$ and that $\mathbf{x}_{R-M}(\Omega_i)$ and $u_{R-M}(\Omega_i)$ do not converge to \mathbf{x}_{∞}^* and u_{∞}^* for $h \rightarrow 0$, as the estimates from Section V indicate. Figures 2b and 3b show that $\|\mathbf{x}_M - \mathbf{x}_{\infty}^*\|_{L^{\infty}}$ and $|u_M - u_{\infty}^*|_{L^2}$ are proportional to $e^{-2\mu_{\infty}T}$, as Lemma 7 indicates. Increasing T increases $\|\mathbf{x}_{R-M}(\Omega_i) - \mathbf{x}_M\|_{L^{\infty}}$ and $|u_{R-M}(\Omega_i) - u_M|_{L^2}$, which confirms that the constant C_T in Theorem 2 increases with T . Figures 2c and 3c show that varying τ does not affect $\|\mathbf{x}_{R-M}(\Omega_i) - \mathbf{x}_M\|_{L^{\infty}}$ and $|u_{R-M}(\Omega_i) - u_M|_{L^2}$ strongly and $\|\mathbf{x}_M - \mathbf{x}_{\infty}^*\|_{L^{\infty}}$ and $|u_M - u_{\infty}^*|_{L^2}$ increase with τ .

The code used to generated the results in this section can be found on <https://github.com/DCN-FAU-AvH>.

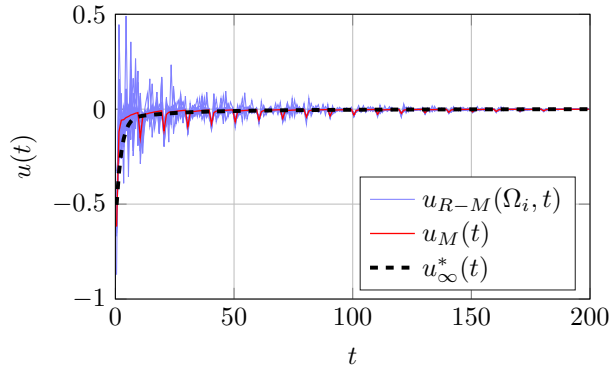
VII. CONCLUSION AND PERSPECTIVES

This paper considers a randomized MPC strategy called RBM-MPC to efficiently approximate the solution of an large-scale infinite-horizon linear-quadratic OCP. In RBM-MPC, the finite-horizon OCPs in each MPC-iteration are simplified by replacing the system matrix A by a randomized one. The estimates in this paper demonstrate that 1) RBM-MPC is stabilizing for $h\text{Var}[A_R]$ sufficiently small and either $T - \tau$ sufficiently large or $\|F - P_{\infty}\|$ sufficiently small, and 2) RBM-MPC states and controls converge in expectation to their MPC counterparts for $h\text{Var}[A_R] \rightarrow 0$. In an example with $n = 100$ states, RBM-MPC is 9 times faster than solving the OCP directly and 3 times faster than classical MPC.

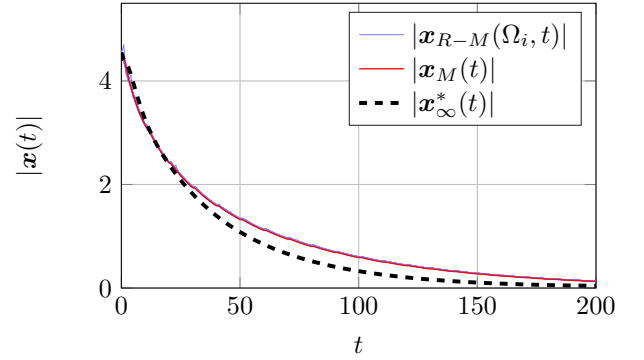
The estimates for the unconstrained linear-quadratic setting in this note form a natural starting point for the analysis of RBM-MPC in nonlinear and/or constrained settings in future works. The computational advantage of RBM-MPC has already been demonstrated in a nonlinear setting, see [7]. Because the training of residual Deep Neural Networks (DNNs) can be seen viewed as a nonlinear OCP (see, e.g., [17], [18]), RBM-MPC may also be applied to speed up the training of DNNs. The numerical example in Section VI also demonstrates the potential advantages of RBM-MPC for the control of (networks of) PDEs, that for example appear in the modeling of gas transport, see, e.g., [19].

Finally, it is worth noting that other variations of RBM-MPC could be considered. One variation would be to first fix a RBM approximation on the whole time axis $[0, \infty)$ and use this as the plant model for MPC, but this variation is less practical to implement than the considered version. Another interesting variation would be to generate a new (independent) RBM approximation in each step of the gradient descent algorithm used to solve the (finite horizon) OCPs in MPC.

- [1] D. Mayne, J. Rawlings, C. Rao, and P. Sokaert, "Constrained model predictive control: Stability and optimality," *Automatica*, vol. 36, no. 6, pp. 789–814, 2000. [Online]. Available: <https://www.sciencedirect.com/science/article/pii/S0005109899002149>
- [2] L. Grüne and J. Pannek, *Nonlinear model predictive control*, ser. Communications and Control Engineering Series. Springer, Cham, 2017, theory and algorithms, Second edition [of MR3155076]. [Online]. Available: <https://doi.org/10.1007/978-3-319-46024-6>
- [3] J. B. Rawlings, D. Q. Mayne, and M. M. Diehl, *Model Predictive Control: Theory, Computation, and Design*. Nob hill publishing, 2019.
- [4] S. Jin, L. Li, and J.-G. Liu, "Random batch methods (RBM) for interacting particle systems," *J. Comput. Phys.*, vol. 400, pp. 108 877, 30, 2020. [Online]. Available: <https://doi.org/10.1016/j.jcp.2019.108877>
- [5] M. Eisenmann and T. Stillfjord, "A randomized operator splitting scheme inspired by stochastic optimization methods," 2022.
- [6] D. W. M. Veldman and E. Zuazua, "A framework for randomized time-splitting in linear-quadratic optimal control," *Numer. Math.*, vol. 151, no. 2, pp. 495–549, 2022. [Online]. Available: <https://doi.org/10.1007/s00211-022-01290-3>
- [7] D. Ko and E. Zuazua, "Model predictive control with random batch methods for a guiding problem," *Math. Models Methods Appl. Sci.*, vol. 31, no. 8, pp. 1569–1592, 2021. [Online]. Available: <https://doi.org/10.1142/S0218202521500329>
- [8] M. Loehning, M. Reble, J. Hasenauer, S. Yu, and F. Allgöwer, "Model predictive control using reduced order models: Guaranteed stability for constrained linear systems," *Journal of Process Control*, vol. 24, no. 11, pp. 1647–1659, 2014.
- [9] J. Lorenzetti, A. McClellan, C. Farhat, and M. Pavone, "Linear reduced-order model predictive control," *IEEE Transactions on Automatic Control*, vol. 67, no. 11, pp. 5980–5995, 2022.

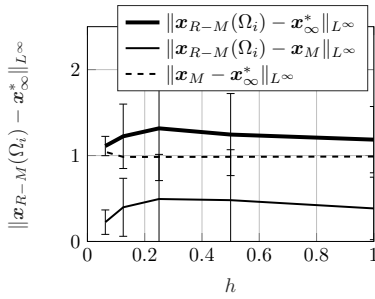


(a) The controls $u_{R-M}(\Omega_i, t)$, $u_M(t)$, and $u_{\infty}^*(t)$.

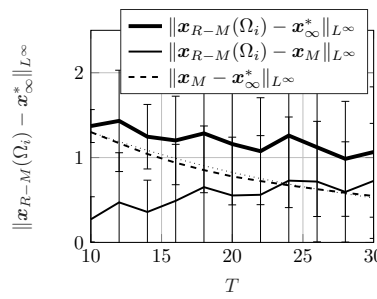


(b) The norm of the state trajectories $x_{R-M}(\Omega_i, t)$, $x_M(t)$, and $x_{\infty}^*(t)$.

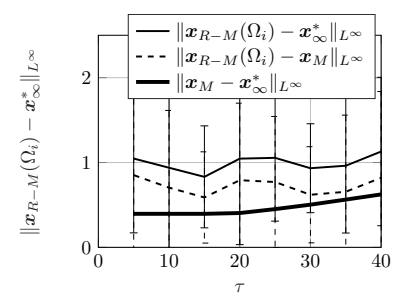
Fig. 1. The RBM-MPC control and state trajectory $u_{R-M}(\Omega_i, t)$ and $x_{R-M}(\Omega_i, t)$ for 20 realizations of Ω_i compared to $u_M(t)$, $x_M(t)$, $u_{\infty}^*(t)$, and $x_{\infty}^*(t)$ for $n = 100$, $h = 1$, $\tau = 10$, and $T = 15$. The lines for $|x_{R-M}(\Omega_i, t)|$ and $|x_M(t)|$ in Figure 1b almost overlap.



(a) Varying h , $T = 15$, $\tau = 10$.

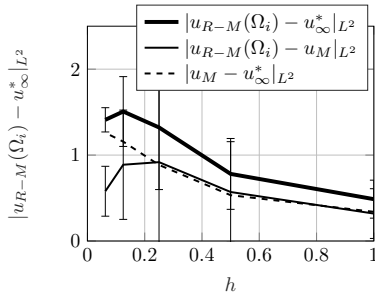


(b) $h = 1$, varying T , $\tau = 10$.

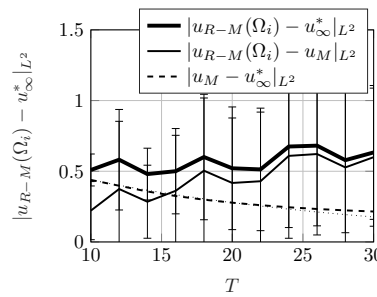


(c) $h = 1$, $T = 40$, varying τ .

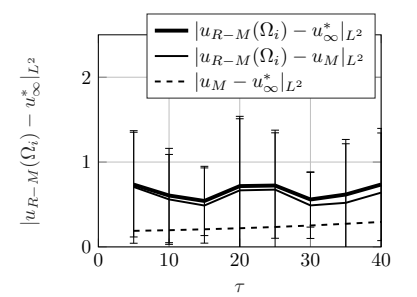
Fig. 2. Differences between the RBM-MPC state trajectory $x_{R-M}(\Omega_i, t)$, the MPC state trajectory $x_M(t)$, and the infinite horizon state trajectory $x_{\infty}^*(t)$ for $n = 100$. The error bars indicate the 2σ confidence intervals estimated based on 20 realizations of Ω_i .



(a) Varying h , $T = 15$, $\tau = 10$.



(b) $h = 1$, varying T , $\tau = 10$.



(c) $h = 1$, $T = 40$, varying τ .

Fig. 3. Differences between the RBM-MPC control $u_{R-M}(\Omega_i, t)$, the MPC control $u_M(t)$, and the infinite horizon control $u_{\infty}^*(t)$ for $n = 100$. The error bars indicate the 2σ confidence intervals estimated based on 20 realizations of Ω_i .

[10] G. Lumer and R. S. Phillips, "Dissipative operators in a banach space," *Pacific Journal of Mathematics*, vol. 11, no. 2, 1961.

[11] A. Quarteroni and A. Valli, *Numerical Approximation of Partial Differential Equations*, ser. Springer Series in Computational Mathematics, 1994, vol. 23.

[12] A. Sage, *Optimum systems control*. Prentice-Hall, Englewood Cliffs, N.J., 1968.

[13] F. M. Callier, J. Winkin, and J. L. Willems, "Convergence of the time-invariant Riccati differential equation and LQ-problem: mechanisms of attraction," *Internat. J. Control*, vol. 59, no. 4, pp. 983–1000, 1994. [Online]. Available: <https://doi.org/10.1080/00207179408923113>

[14] A. Porretta and E. Zuazua, "Long time versus steady state optimal control," *SIAM J. Control Optim.*, vol. 51, no. 6, pp. 4242–4273, 2013. [Online]. Available: <https://doi.org/10.1137/130907239>

[15] V. K. Rohatgi and A. K. M. E. Saleh, *An introduction to probability and statistics*, 3rd ed., ser. Wiley Series in Probability and Statistics.

John Wiley & Sons, Inc., Hoboken, NJ, 2015. [Online]. Available: <https://doi.org/10.1002/9781118799635>

[16] T. Apel and T. G. Flaig, "Crank-Nicolson schemes for optimal control problems with evolution equations," *SIAM J. Numer. Anal.*, vol. 50, no. 3, pp. 1484–1512, 2012. [Online]. Available: <https://doi.org/10.1137/100819333>

[17] M. Benning, E. Celledoni, M. J. Ehrhardt, B. Owren, and C.-B. Schönlieb, "Deep learning as optimal control problems: models and numerical methods," *J. Comput. Dyn.*, vol. 6, no. 2, pp. 171–198, 2019. [Online]. Available: <https://doi.org/10.3934/jcd.2019009>

[18] C. Esteve, B. Geshkovski, D. Pighin, and E. Zuazua, "Large-time asymptotics in deep learning," 2020. [Online]. Available: <https://arxiv.org/abs/2008.02491>

[19] M. Herty, "Modeling, simulation and optimization of gas networks with compressors," *New. Heterog. Media*, vol. 2, no. 1, pp. 81–97, 2007. [Online]. Available: <https://doi.org/10.3934/nhm.2007.2.81>